Sensors and Actuators B 230 (2016) 559–565

Contents lists available at ScienceDirect

Sensors and Actuators B: Chemical

journal homepage: www.elsevier.com/locate/snb

Highly sensitive non-enzymatic electrochemical glucose biosensor using a photolithography fabricated micro/nano hybrid structured electrode

Che-Wei Hsu[a], Fang-Ci Su[a], Po-Yu Peng[b], Hong-Tsu Young[c], Stephen Liao[b], Gou-Jen Wang[a,d,*]

[a] Department of Mechanical Engineering, National Chung-Hsing University, Taichung 402, Taiwan
[b] Phoenix Silicon International Corporation, Hsinchu 300, Taiwan
[c] Department of Mechanical Engineering, National Taiwan University, Taipei 106, Taiwan
[d] Graduate Institute of Biomedical Engineering, National Chung-Hsing University, Taichung 402, Taiwan

ARTICLE INFO

Article history:
Received 2 November 2015
Received in revised form 2 February 2016
Accepted 22 February 2016
Available online 24 February 2016

Keywords:
Non-enzymatic glucose biosensor
Micro/nano hybrid structured electrode
Photolithography

ABSTRACT

In this study, a novel non-enzymatic glucose biosensor based on a simple photolithographic process is proposed. To fabricate the sensor, photoresist AZ-1518 was spin-coated onto a reclaimed silicon wafer, and then, a mask with a hexagonal close-packed circle array was employed for exposure and development to generate a hexagonal close-packed column array of AZ-1518. The diameter of each circle was set as 3 μm. Subsequently, a thermal melting process was employed to convert each photoresist column into a photoresist hemisphere. A gold thin film was then sputtered onto the hemisphere array of AZ-1518 to form the sensing electrode. Finally, gold nanoparticles were deposited onto the gold thin film using a self-assembly monolayer method to enhance the sensing area. Measurements showed a 10.2-fold enhancement of the sensing area in comparison with a plain gold electrode. Actual detection of glucose demonstrated that the proposed non-enzymatic glucose biosensor can operate in a linear range of 55.6 μM–13.89 mM. It had a sensitivity of 749.2 $\mu A\,mM^{-1}\,cm^{-2}$ and a detection limit of 9 μM. The novel glucose biosensor proposed here has several advantages such as being enzyme free, simple to fabricate, low cost, and easy to preserve on a long-term basis. Thus, it can feasibly be used for future clinical applications.

1. Introduction

Diabetes is now a severe global public health problem. It can be classified into two main types: type 1 diabetes mellitus (T1DM) and type 2 diabetes mellitus (T2DM). T1DM is caused by the insufficient production of insulin in the pancreas, whereas T2DM occurs when the body does not make full use of the insulin produced by the pancreas [1]. As of 2015, the International Diabetes Federation reported that approximately 387 million people worldwide suffer from diabetes, with 90% of the cases suffering from T2DM [2,3]. Regular detection of a diabetes patient's blood glucose is essential for effectively maintaining their blood sugar level.

Various techniques have been proposed for continuous glucose monitoring. In general, electrochemical and optical approaches are the most commonly used methodologies [4]. Electrochemical sensors make up the majority of commercially available glucose-sensing devices because of their practicability, simplicity, and low cost [5,6]. Electrochemical-based sensors can be classified according to the use of enzymatic and non-enzymatic approaches. In enzymatic approaches, glucose is oxidized to gluconolactone, with the reaction catalyzed by the glucose-specific enzyme glucose oxidase (GOx). In non-enzymatic approaches, glucose is directly oxidized to gluconolactone at nanostructured electrodes that provide a large reaction area for effective electrocatalytic activity. The advantages of enzymatic approaches include their high response to glucose and good specificity of glucose detection [7–9]; however, the inevitable disadvantages include the relatively complicated and multistep immobilization processes, chemical and thermal instability, and degradation of the GOx. Therefore, non-enzymatic approaches, which do not require an immobilization procedure, are free from the degradation problem, and have high stability,

* Corresponding author. Fax: +886 4 22877170.
E-mail address: gjwang@dragon.nchu.edu.tw (G.-J. Wang).

http://dx.doi.org/10.1016/j.snb.2016.02.109
0925-4005/

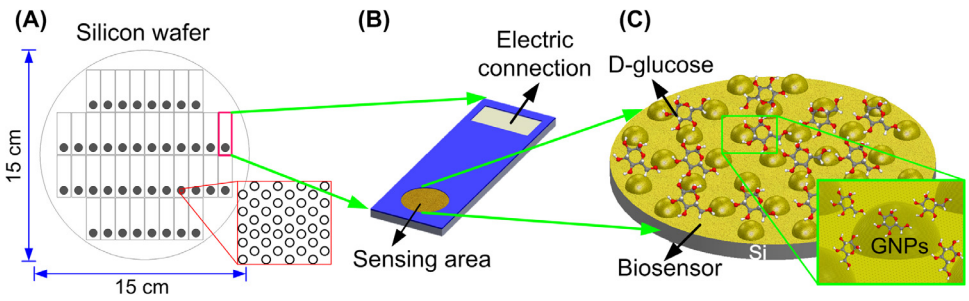

Fig. 1. Schematic of the proposed novel non-enzymatic biosensor. (A) Mask layout, (B) sensor packing, and (C) sensing electrode with a micro/nano hybrid structure.

simplicity, and reproducibility, have recently attracted increasing attention [10,11].

Gold is generally recognized as an inert metal since electrons fill the *d* orbitals. Therefore, in electro-oxidation, gold is usually considered as a poor substrate to absorb the participating species of organic substances, such as glucose. However, nanoscale gold materials, which have catalytic mechanisms similar to natural GOx, can provide a strong catalytic activity [12]. Because gold is an inert metal, a glucose biosensor based on a gold substrate is more stable given variations in pH and temperature. Feng et al. developed a non-enzymatic glucose sensor using a glassy carbon electrode (GCE) coated with a chitosan-gold nanoparticles (GNPs) nanocomposite-sensing film [13]. This sensor produced a linear performance in the concentration range from 400 μM to 10.7 mM and had a 370-μM limit of detection. Li et al. employed specific boronic acid-diol binding to develop a non-enzymatic platform for glucose sensing [14]. They used a GNPs-Prussian blue (GNPs-PB) nanocomposite deposited on a gold electrode surface as the electrochemical indicator. A second GNP layer was deposited on the GNPs-PB nanocomposite surface to further improve the sensitivity of the sensor. The sensor had a linear detection range of 0.1–13.5 μM and a 0.05-μM detection limit.

Besides the use of GNPs for glucose detection, other gold nanostructures have also been applied to glucose biosensors. In one study, urchin-like gold submicrostructures, which have better catalytic activity for glucose oxidation than flower-like gold submicrostructures, and Nafion solution were cast onto a GCE for non-enzymatic glucose detection [15]. The linear detection range, sensitivity, and detection limit were measured as 0.2–13.2 mM, 16.8 $\mu A\,mM^{-1}\,cm^{-2}$, and 10 μM, respectively. Chen et al. reported a non-enzymatic electrochemical glucose biosensor based on nanoporous gold (NPG) [16]. Since silver can be etched off by a HNO_3 solution, such a solution was employed to etch off the $Au_{35}Ag_{65}$ (at.%) alloy of Ag to form a NPG film and then to directly sense glucose concentration. The linear range, sensitivity, and detection limit of this sensor were measured as 1–18 mM, 20.1 $\mu A\,mM^{-1}\,cm^{-2}$, and 800 nM, respectively. Shu et al. proposed a dendrite-like electrode of gold nanostructures (DGNs) to directly detect glucose levels [17]. The electrode was immersed in a $HAuCl_4$ solution and a potential was applied to form DGNs on a GCE. This electrode had a wide linear detection range of 0.1–25 mM, a high sensitivity of 190.7 $\mu A\,mM^{-1}\,cm^{-2}$, and a low detection limit of 0.05 μM. Cherevko and Chung investigated a gold nanowire array electrode for use as a non-enzymatic glucose biosensor [18]. Specifically, a gold nanowire array was deposited on an anodic aluminum oxide (AAO) template, and then the AAO template was removed using a NaOH solution to obtain a nanowire structure array. The linear detection range of this device was 0.5–14 mM, while the sensitivity and detection limit were 309 $\mu A\,mM^{-1}\,cm^{-2}$ and 30 μM, respectively. In addition to the pure gold-based sensors, composite metals have recently been studied and used in non-enzymatic glucose biosensors. For example, Shen et al. proposed a bimetallic Pd–Au cluster non-enzymatic glucose biosensor that was synthesized through a direct chemical reduction method [19]. This sensor demonstrated a linear range of 0.1–13.5 μM, a sensitivity of 75.3 $\mu A\,mM^{-1}\,cm^{-2}$, and a detection limit of 50 μM.

The trend for development of in vitro diagnosis devices requires that these devices be low cost, sensitive, specific, easy to use, and disposable. For the current non-enzymatic glucose detection techniques, a relatively complicated and time-consuming nanomaterial

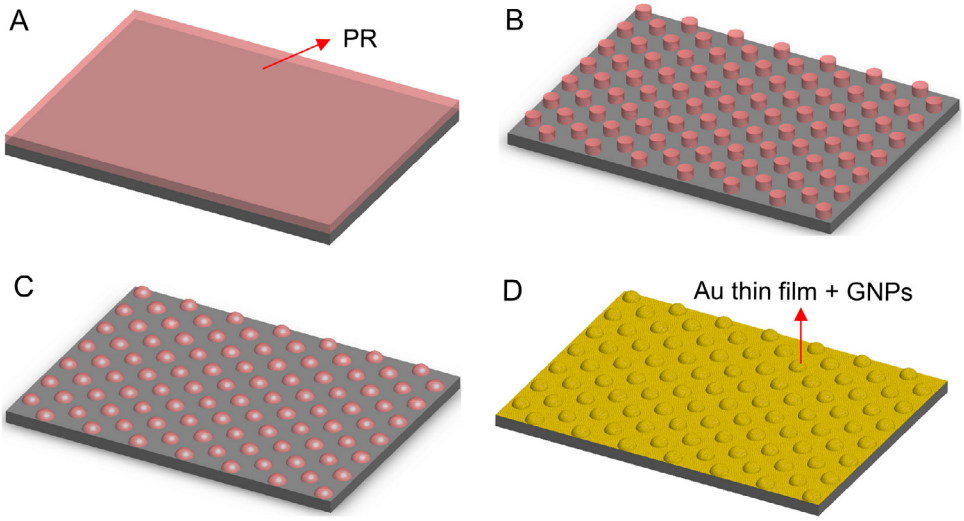

Fig. 2. Schematic of the fabrication procedure. (A) Silicon-wafer cleaning and positive photoresist coating, (B) exposure and development, (C) thermal melting, and (D) gold thin film sputtering and deposition of GNPs.

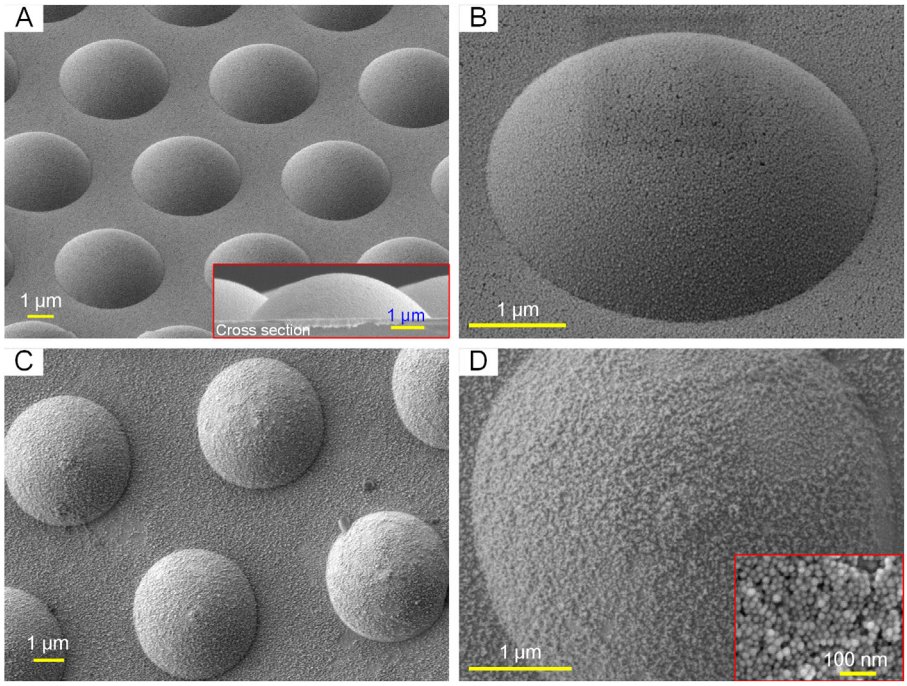

Fig. 3. Scanning electron microscopy images of the wafer at different fabrication steps. (A) After Au sputtering (inset: a cross sectional view). (B) High magnification of a single hemisphere. (C) After GNP deposition. (D) Magnified image of a single hemisphere after GNP deposition.

preparation process is required; thus, the commercial application of these sensors is limited. In the present study, a novel non-enzymatic glucose biosensor produced using a simple lithographic process is proposed. Specifically, photoresist AZ-1518 was spin-coated onto a reclaimed silicon wafer. A mask with a hexagonal close-packed circle array was then employed for exposure and development to generate a hexagonal close-packed column array of the AZ-1518. A thermal melting process was than conducted to convert each photoresist column into a photoresist hemisphere. Finally, a gold thin film was sputtered onto the hemisphere array of AZ-1518 to form the sensing electrode.

2. Materials and methods

Fig. 1 schematically illustrates the photolithographic process for the proposed non-enzymatic glucose biosensor. Fig. 1(A) shows the mask layout for 6 in. silicon wafer. This mask contains 40 cycles (φ = 8 mm, the centre-to-centre distance between two neighboring discs is 10 mm) with each cycle containing over 2 million hexagonal close-packed small circles (φ = 3 μm, the centre-to-centre distance between two neighboring cycles is 6 μm). Following the photolithographic process, thermal melting process, and gold thin film sputtering, the wafer was cut into forty $1 \times 1\ cm^2$ rectangles, with each rectangle containing a cycle. Each rectangular sample was then packaged on a glass slide (as shown in Fig. 1(B)). GNPs were deposited on the gold thin film electrode surface to complete the simple lithographic non-enzymatic glucose biosensor. Fig. 1(C) illustrates the schematic enlargement of sensing area. The sensor electrode, which was composed of micro- and nano-structures, could directly respond to glucose without any GOx and mediator.

2.1. Sensor fabrication

Fig. 2 shows a schematic description of the sequential fabrication procedures for the proposed simple non-enzymatic glucose biosensor, including silicon wafer cleaning and photoresist coating, exposure and development, thermal melting, and gold thin film sputtering and deposition of GNPs. The full details are described below.

(1) Silicon wafer cleaning and photoresist coating

Reclaimed 6-in. silicon wafers (700 μm thick; Phoenix Silicon International, Taiwan) were used in this study. Each wafer was ultrasonically cleaned in acetone, EtOH, and deionized water in turn for 20 min in each solution. After ultrasonic cleaning, the wafer was blown with nitrogen to clear up obvious water drips, and then placed on a 150 °C hot plate for 2 min to remove residual moisture.

First, the wafer was coated with hexamethyldisilazane (HMDS) to enhance the adhesion between the wafer surface and the coated photoresist. Positive photoresist (PR) AZ 1518 was subsequently spin-coated onto the wafer. The parameters used for the spin coating were as follows: spinning speed of the first stage = 500 rpm, spinning time for the first stage = 10 s, spinning speed of the second stage = 1500 rpm, and spinning time for the second stage = 40 s. The PR-coated wafer was soft baked at 100 °C for 90 s.

(2) Exposure and development

For exposure, a mask aligner (EVG 620, wavelength = 400 nm) was used for 9.5 s to transfer the desired pattern to the PR layer. Subsequently, development was conducted for 2 min using a 2.38% TMAH developer. As depicted in Fig. 2(B), an array of photoresist columns was obtained.

(3) Thermal melting

Due to the surface tension effect, a photoresist column becomes a hemisphere (Fig. 2(C)) after thermal melting, which gradually increases the ambient temperature above the glass transition temperature (T_g) of the photoresist. In this study, thermal melting was used to convert the column array of photoresist into a hemisphere array of photoresist, which enabled the uniform sputtering of the gold thin film electrode. The thermal melting was performed using

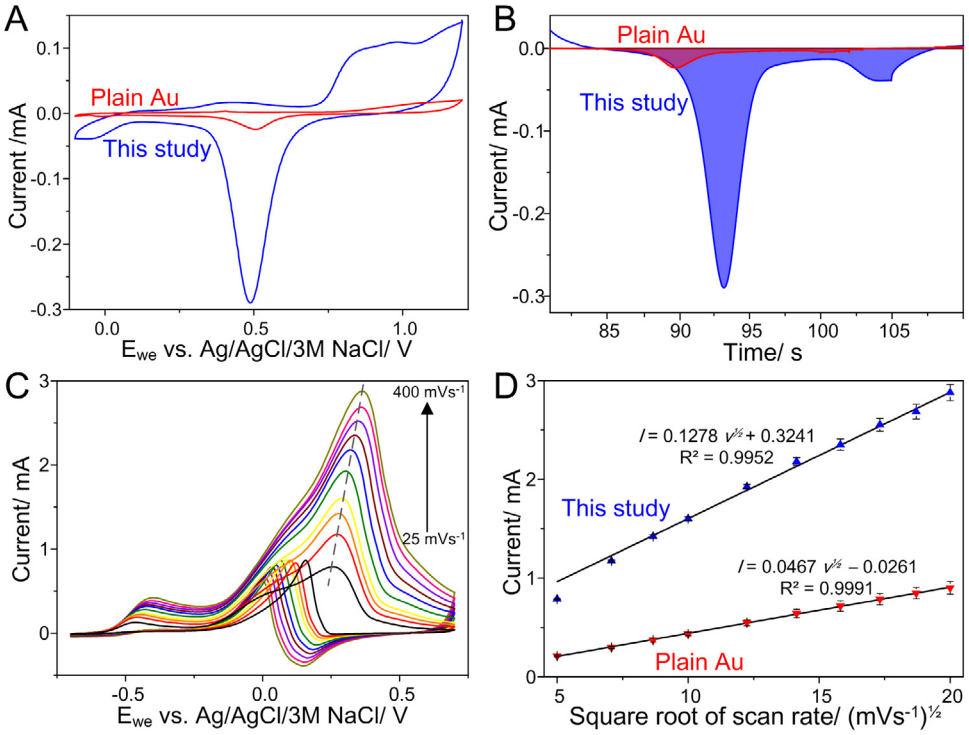

Fig. 4. The proposed electrode characterized by cyclic voltammetry. (A) Cyclic voltammetry (i–v) with a scan rate of 50 mV s^{-1} in a 0.1-M phosphate buffer solution (pH 7.0). (B) The corresponding current versus time (i–t) curves. (C) Cyclic voltammetry with various scan rates (25, 50, 75, 100, 150, 200, 250, 300, 350, and 400 mV s^{-1}) in a 0.1-M NaOH solution containing 5.56 mM of glucose electrolytes. (D) Linear relationship between the redox peak current and the square root of the scan rate.

a hot plate. Since the T_g of AZ-1518 is around 130 °C, the temperature of the hot plate was gradually increased to 150 °C in 5 min.

(4) Gold thin film sputtering and deposition of GNPs

After thermal melting, the wafer was diced into small pieces ($1 \times 1\,cm^2$) to fit the sputter chamber. A gold thin film was deposited onto the sample surface by sputtering using a sputter coater (Model 108 Auto, Cressington). The target of sputter is gold (99.99%), and the max power of the sputter machine is 500 W. The relevant processes are described below: The samples were put in the sputter chamber, and the chamber was started evacuating to vacuum (0.08 mbar). Then Argon gas was continuously microinjected into chamber, and the flow of Argon gas was adjusted to keep the chamber pressure at 0.08 mbar. The sputter current and period are set as 30 mA and 135 s, respectively. Finally, the gold thin film was deposited on the sample surface. To ensure the uniformity of the sputtered gold thin film, the samples were heated in an oven to 120 °C at a rate of 5 °C/min, with the temperature maintained for 80 min. Finally, the sample was cooled to room temperature.

To assure the consistency of the sensing area, the gold thin film sputtered electrode was packaged. First, a conductive silver wire was attached to a glass slide as the conducting wire. Then, a $2 \times 2\,cm^2$ square of Parafilm with a hole ($\varphi = 6$ mm) was bonded to the sample to cover the non-sensing area (as shown in Fig. 1(B)).

The GNPs were prepared using the well-known reduction method [20]. First, 100 mL of 0.01% $HAuCl_4$ solution was stirred and heated to boiling point, and then 4 mL of 1% sodium citrate was added and continuously stirred for 10 min. After 10 min, heating was stopped and the solution was allowed to cool to room temperature. The pH value of the solution was then adjusted to 11 using a NaOH solution to increase the spacing between GNPs. Subsequently, 1.5 mL of 10 mM 11-mercaptoundecanoic acid 95% (MUA) was added to this solution and ultrasonically mixed for 20 min. The gold colloidal solution was then added to a centrifuge tube and centrifuged at 15,000 rpm for 15 min. After centrifugation, the precipitate was collected in a container and stored in the dark. The packaged electrode was immersed in a solution composed of 1 mL 3-aminopropyltrimethoxysilane 97% (APTMS), 1 mL ethanol, and 18 mL distilled deionized (DDI) water for 12 h to ensure that the APTMS completely attached to the electrode surface. The electrode was sequentially rinsed with DDI water, blown with nitrogen, and placed on a hot plate heated to 50 °C. Next, 20 μL of concentrated GNP solution was dripped onto the electrode and it was incubated for 30 min. The electrode was then rinsed with DDI water to wash off the non-attached GNPs, and it was blown with nitrogen until dry (Fig. 2(D)). Finally, the fabricated non-enzymatic glucose biosensor was stored in the dark at room temperature until further use.

2.2. Sensor characterization

The morphologies of the fabricated array electrode of the hemisphere were characterized using a field emission gun scanning electron microscopy (JSM-6700F, JEOL, Japan). A SP-150 potentiostat (Bio-Logic, USA) was applied for the electrochemical experiments. Cyclic voltammetry (CV) was conducted in a 0.1-M phosphate buffer solution (pH 7.0) to estimate the real sensing area of the electrode. Glucose concentrations were measured using CV and amperometry approaches in a 0.1-M NaOH solution (pH 7.4).

3. Results and discussion

Fig. 3 illustrates the fabrication results of the sensor at different fabrication steps. Fig. 3(A) displays the 45° view of a hemispheric array that has undergone the Au sputtering process. Thermal melting successfully converted the column array of photoresist into a

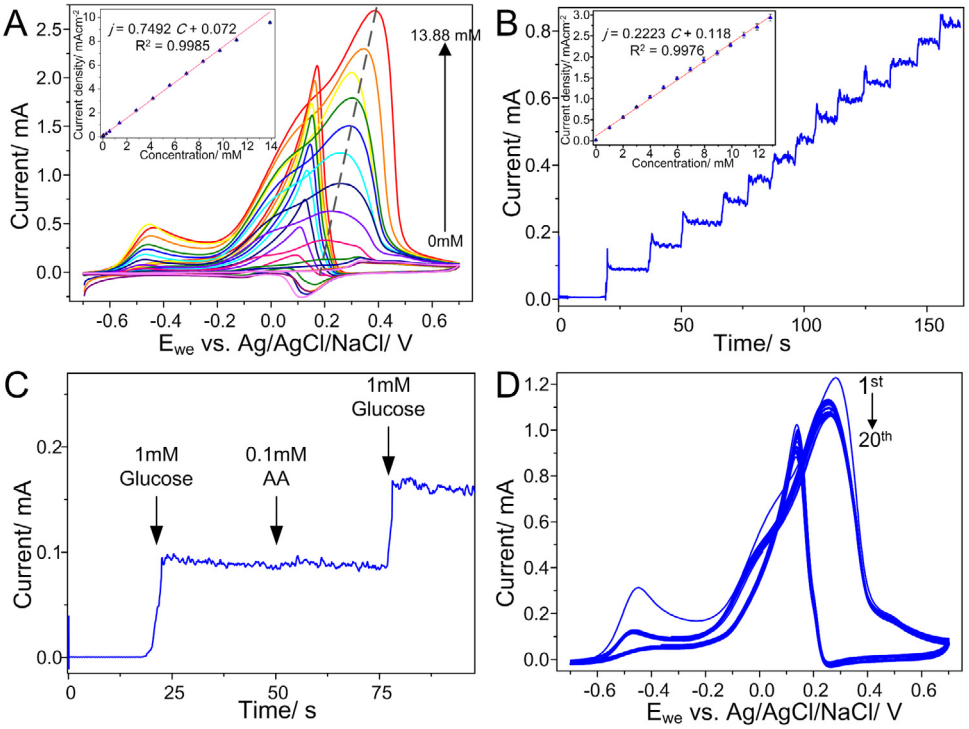

Fig. 5. Glucose detection results. (A) Cyclic voltammograms (50 mV s^{-1}) for various glucose concentrations with curves representing the concentrations (0, 0.06, 0.28, 0.56, 1.39, 2.78, 4.16, 5.56, 6.94, 8.32, 9.71, 11.10, and 13.89 mM). The inset shows a linear calibration curve representing the peak current and concentration relationship. (B) The amperometry result for successive addition of 1 mM glucose (applied potential was 0.1 V). The inset shows the corresponding calibration curve. (C) Response to sequential injections of 1 mM glucose, 0.1 mM ascorbic acid (AA), and 1 mM glucose. (D) Stability of cyclic voltammetry in a 0.1-M NaOH solution containing 5.56 mM glucose for 20 cycles.

hemispheric array. The height of each hemisphere was about 2 μm, as illustrated in the inset of Fig. 3(A). The hemispheres were also uniformly distributed. Fig. 3(B) shows a highly magnified image of one hemisphere; the diameter of the hemisphere was approximately 4 μm. Due to surface tension and hydrophilicity, the area of the patterned PR base would be slightly expanded after thermal melting. Fig. 3(C) and (D) shows the morphologies of part of the array and a single hemisphere after GNP deposition, respectively. The results indicate that GNPs were uniformly deposited on the electrode surface and the hemisphere's shape remained intact. The size of GNPs was estimated as about 20 nm (as shown in the inset of Fig. 3(D)).

It has been reported that a rough electrode surface could enhance the sensitivity of a biosensor [21,22]. The electrode surface of the proposed non-enzymatic glucose sensor was rougher than that of a flat gold electrode. The roughness of an electrode is defined by the value of the true area divided by the geometric surface area. CV can be used to estimate the true area in terms of the amount of oxide reduction on the gold electrode surface [23,24].

Fig. 4(A) shows the cyclic voltammograms of the proposed electrode and a plain gold electrode, while the corresponding current versus time (i–t) curves are shown in Fig. 4(B). The area below the horizontal axis (zero current) (as shown in Fig. 4(B)) represents the total electric charges required for a complete reduction on the electrode. For the proposed electrode and the plain gold electrode, the area below the horizontal axis were 1120.6 μC and 109.5 μC, respectively. Since a total charge of 390 μC was required for 1 cm^2 of the Au electrode to form AuO, the effective sensing area of the proposed electrode was estimated as 2.873 cm^2 (1120.6 μC/390 μC). This area is approximately 10.2-fold greater than the geometric area (0.283 cm^2).

The kinetics of partial oxidation of glucose on the proposed simple photolithographic-based biosensor was determined by CV measurements with various scan rates. Fig. 4(C) displays the cyclic voltammograms of the proposed electrode for various scan rates from 25 to 400 mV s^{-1} in a 0.1-M NaOH solution containing 5.56 mM of glucose electrolytes. The peak currents and peak potentials increased with increasing scan rate. A typical diffusion-controlled reaction can be confirmed by the Randles–Sevcik equation, which is as follows:

$$i_p = 2.69 \times 10^5 \times n^{3/2} \times A \times C \times D^{1/2} \times v^{1/2} \quad (1)$$

where i_p indicates the value of peak current (A), n denotes the number of electrons appearing in a half-reaction for the redox couple, A is the electrode area (cm^2), C is the concentration of the analyte (mol/cm^3), D is the diffusivity of the analyte (cm^2/s), and v represents the potential scan rate (V/s). Assuming n, A, C, and D are fixed, i_p is proportional to the square root of the scanning rate.

The linear relationships between the peak current and the scan rate of the proposed biosensor are depicted in Fig. 4(D). The peak current was found to be highly and linearly associated with the square root of the scan rate. Thus, the proposed biosensor exhibited typical diffusion-controlled electrochemical behavior that would be suitable for applications involving practical quantitative analysis. Furthermore, the slope of the Randles–Sevcik line for our proposed biosensor was 2.7-fold greater than that of a plain gold electrode. The inconsistence of the increases between the slope of the Randles–Sevcik line and the sensing area can be attributed to the diffusion limitation [25].

To precisely demonstrate the glucose detection performance of the proposed biosensor, various experiments were performed and the results are illustrated in Fig. 5. Fig. 5(A) shows the cyclic voltammograms (50 mV/s) in a 0.1-M NaOH solution for various glucose concentrations (0–13.89 mM). We observed three evident current peaks whose values were proportional to glucose concentrations. The first peak, located at ~−0.45 V, represents the

Table 1
Nanostructure-based non-enzymatic glucose biosensors and their functional properties.

Electrode	Sensitivity ($\mu A\,mM^{-1}\,cm^{-2}$)	LOD (μM)	Linear range (mM)	Reference
Chitosan/GNPs/GCE	Not provided	370	0.4–10.7	[13]
GNPs–PB/GE	Not provided	0.05	0.0001–0.0135	[14]
Nafion–UGS/GCE	16.8	10	0.2–13.2	[15]
Nanoporous Au	20.1	3	1.0–18.0	[16]
Gold nanostructure/GCE	190.7	0.05	0.1–25	[17]
Gold nanowire array	309	50	0.5–14	[18]
Pd–Au cluster	75.3	50	0.1–30	[19]
Micro/nano hybrid structured biosensor	749.2	9	0.0556–13.89	This work

formation and adsorption of intermediate compounds. The other two peaks, located at ~0.1 and ~0.25 V, characterize the direct oxidation of glucose in the cathodic and anodic direction, respectively [18].

We also rearranged the data displayed in Fig. 5(A) and plotted the relationships between each peak current (the potential at 0.25 V) and its corresponding glucose concentration (see the inset of Fig. 5(A)). Each measurement was repeated five times. The linear detection range was 55.56 μM–13.89 mM with a high R^2 value of 0.9985. The sensitivity of the proposed glucose biosensor was calculated as 749.2 $\mu A\,mM^{-1}\,cm^{-2}$ and the detection limit was 9 μM. The high sensitivity can be ascribed to the large effective sensing area of the proposed biosensor, which enables the oxidization of a considerable amount of glucose.

Fig. 5(B) displays the amperometry result for successive addition of 1 mM glucose to our proposed non-enzymatic glucose biosensor. The sensor was immersed in a continuously stirred 0.1-M NaOH solution and a constant potential of 0.1 V was applied. Subsequently, 1 mM of glucose was periodically added to the solution and the trajectories of the current along with the processing time were recorded. The amperometric currents increased rapidly with each addition of glucose. We also rearranged the measured current of each stepwise and its corresponding glucose concentration, and we plotted the curve in the inset of Fig. 5(B). The calibration curve was linear proportional to glucose concentrations in the range of 1–13 mM, with a correlation coefficient of 0.9976.

Interference of other substances such as ascorbic acid (AA) in human blood can degrade the efficacy of a glucose-sensing device because the concentration of glucose in a normal human (3–8 mM) is much higher than the interference concentration (~0.1 mM) [19]. In this investigation, the ratio of glucose and AA concentrations was decreased to 10 to demonstrate the selectivity performance of the proposed biosensor. The response of the proposed biosensor to sequential injections of 1 mM glucose, 0.1 mM AA, and 1 mM glucose in a 0.1-M NaOH solution under an operating potential of 0.1 V was investigated, and the corresponding results are illustrated in Fig. 5(C). We found that the proposed biosensor was hardly influenced by AA interference.

In addition to linear range, detection limit, sensitivity, and selectivity, stability is another key feature of a glucose biosensor. To investigate the stability of the proposed biosensor, it was repetitively tested through 20CV cycles using the electrolyte of a 0.1-M NaOH solution containing 5.56 mM of glucose. The corresponding results are presented in Fig. 5(D). The peaks of the first CV scan were higher than subsequent scans. Since the electrolyte was not stirred, the response of glucose oxidation was the strongest and the most rapid in the first scan. After the first CV scan, the glucose in the vicinity of the electrode surface was reacted and consumed, which resulted in the decreasing response observed in subsequent scans. Nevertheless, after the second scan, the peak currents varied only slightly. Since the glucose was continuously diffused to the electrode surface and the diffusion and reaction speed was approximately the same, the responses slightly varied in subsequent scans. In addition, the detection performances of proposed biosensors that were stored in air at room temperature for over 2 months remained practically constant.

In recent years, nanostructured electrodes have been widely used in diabetes detection devices because of their beneficial characteristics, which include their large surface area, high surface activity, high catalytic efficiency, and strong adsorption capacity. In Table 1, the functional properties of the proposed non-enzymatic glucose biosensor are compared with those of other recently developed non-enzymatic glucose biosensors in terms of sensitivity, detection limit, and linear range. Overall, the biosensor proposed in this study exhibited relatively good functional properties.

4. Conclusion

Diabetes is a serious worldwide public health problem, with approximately 387 million people suffering from the disease. Diabetics must frequently monitor their own blood sugar levels to ensure their blood sugar concentrations are maintained within an appropriate range. In this study, we proposed a novel non-enzymatic glucose biosensor based on a simple lithographic process. The sequential process for fabrication of the proposed electrode included the following steps: (1) spin-coating photoresist AZ-1518 onto a reclaimed silicon wafer, (2) using a mask with a hexagonal close-packed circle array for exposure and development to produce a hexagonal close-packed column array of photoresist AZ-1518, (3) thermal melting to convert each photoresist column into a photoresist hemisphere, and (4) sputtering a gold thin film and GNPs onto the hemisphere array of AZ-1518 to form the sensing electrode. The effective sensing area of the proposed electrode was found to be 10.2-fold greater than that of a corresponding plain gold electrode. Actual glucose measurements revealed that the proposed biosensing scheme could operate in a linear range of 55.56 μM–13.89 mM with a sensitivity of 749.2 $\mu A\,mM^{-1}\,cm^{-2}$ and a detection limit of 9 μM. The stability of our proposed non-enzymatic glucose biosensor was confirmed through 20 cycles of CV and a follow-up investigation over 2 months. The proposed novel non-enzymatic glucose biosensor has the advantages of being enzyme free, simple to fabricate, low cost, and easy to preserve on a long-term basis. Therefore, it is feasible that, in the future, the biosensor could be commercialized and used in clinical applications.

Acknowledgement

The authors would like to offer their thanks to the Ministry of Science and Technology of Taiwan under grant number (MOST-103-2622-E-005-012-CC2) for their financial support of this research.

References

[1] E. Kitabchi, G.E. Umpierrez, J.M. Miles, J.N. Fisher, Hyperglycemic crises in adult patients with diabetes, Diabetes Care 32 (2009) 1335–1343.
[2] S. Melmed, K.S. Polonsky, P.R. Larsen, H.M. Kronenberg, Williams Textbook of Endocrinology: Expert Consult, Elsevier Health Sciences, 2011.

[3] Y. Shi, F.B. Hu, The global implications of diabetes and cancer, Lancet 383 (2014) 1947–1948.
[4] S. Vaddiraju, D.J. Burgess, I. Tomazos, F.C. Jain, F. Papadimitrakopoulos, Technologies for continuous glucose monitoring: current problems and future promises, J. Diabetes Sci. Technol. 4 (2010) 1540–1562.
[5] X. Bo, J. Bai, L. Yang, L. Guo, The nanocomposite of PtPd nanoparticles/onion-like mesoporous carbon vesicle for nonenzymatic amperometric sensing of glucose, Sens. Actuators B: Chem. 157 (2011) 662–668.
[6] B. He, L. Hong, J. Lu, J. Hu, Y. Yang, J. Yuan, et al., A novel amperometric glucose sensor based on PtIr nanoparticles uniformly dispersed on carbon nanotubes, Electrochim. Acta 91 (2013) 353–360.
[7] X. Kang, J. Wang, H. Wu, I.A. Aksay, J. Liu, Y. Lin, Glucose oxidase–graphene–chitosan modified electrode for direct electrochemistry and glucose sensing, Biosens. Bioelectron. 25 (2009) 901–905.
[8] C. Wu, H. Sun, Y. Li, X. Liu, X. Du, X. Wang, et al., Biosensor based on glucose oxidase-nanoporous gold co-catalysis for glucose detection, Biosens. Bioelectron. 66 (2015) 350–355.
[9] C.W. Hsu, W.C. Feng, F.C. Su, G.J. Wang, An electrochemical glucose biosensor with a silicon nanowire array electrode, J. Electrochem. Soc. 162 (2015) B264–B268.
[10] J. Wang, Electrochemical glucose biosensors, Chem. Rev. 108 (2008) 814–825.
[11] S. Park, H. Boo, T.D. Chung, Electrochemical non-enzymatic glucose sensors, Anal. Chim. Acta 556 (2006) 46–57.
[12] G. Wang, X. He, L. Wang, A. Gu, Y. Huang, B. Fang, et al., Non-enzymatic electrochemical sensing of glucose, Microchim. Acta 180 (2013) 161–186.
[13] D. Feng, F. Wang, Z. Chen, Electrochemical glucose sensor based on one-step construction of gold nanoparticle–chitosan composite film, Sens. Actuators B: Chem. 138 (2009) 539–544.
[14] J. Li, Z. Wang, P. Li, N. Zong, F. Li, A sensitive non-enzyme sensing platform for glucose based on boronic acid-diol binding, Sens. Actuators B: Chem. 161 (2012) 832–837.
[15] F. Xu, K. Cui, Y. Sun, C. Guo, Z. Liu, Y. Zhang, et al., Facile synthesis of urchin-like gold submicrostructures for nonenzymatic glucose sensing, Talanta 82 (2010) 1845–1852.
[16] L. Chen, X. Lang, T. Fujita, M. Chen, Nanoporous gold for enzyme-free electrochemical glucose sensors, Scr. Mater. 65 (2011) 17–20.
[17] H. Shu, L. Cao, G. Chang, H. He, Y. Zhang, Y. He, Direct electrodeposition of gold nanostructures onto glassy carbon electrodes for non-enzymatic detection of glucose, Electrochim. Acta 132 (2014) 524–532.
[18] S. Cherevko, C.-H. Chung, Gold nanowire array electrode for non-enzymatic voltammetric and amperometric glucose detection, Sens. Actuators B: Chem. 142 (2009) 216–223.
[19] C. Shen, J. Su, X. Li, J. Luo, M. Yang, Electrochemical sensing platform based on Pd–Au bimetallic cluster for non-enzymatic detection of glucose, Sens. Actuators B: Chem. 209 (2015) 695–700.
[20] I.C. Ni, S.C. Yang, C.-W. Jiang, C.S. Luo, W. Kuo, K.J. Lin, et al., Formation mechanism, patterning, and physical properties of gold-nanoparticle films assembled by an interaction-controlled centrifugal method, J. Phys. Chem. C 116 (2012) 8095–8101.
[21] H. Qiu, L. Xue, G. Ji, G. Zhou, X. Huang, Y. Qu, et al., Enzyme-modified nanoporous gold-based electrochemical biosensors, Biosens. Bioelectron. 24 (2009) 3014–3018.
[22] E. Seker, M.L. Reed, M.R. Begley, Nanoporous gold: fabrication, characterization, and applications, Materials 2 (2009) 2188–2215.
[23] E.F. Douglass Jr., P.F. Driscoll, D. Liu, N.A. Burnham, C.R. Lambert, W.G. McGimpsey, Effect of electrode roughness on the capacitive behavior of self-assembled monolayers, Anal. Chem. 80 (2008) 7670–7677.
[24] S. Trasatti, O. Petrii, Real surface area measurements in electrochemistry, J. Electroanal. Chem. 327 (1992) 353–376.
[25] M.D. Scanlon, U. Salaj-Kosla, S. Belochapkine, D. MacAodha, D. Leech, Y. Ding, E. Magner, Characterization of nanoporous gold electrodes for bioelectrochemical applications, Langmuir 28 (2012) 2251–2261.

Biographies

Dr. Che-Wei Hsu received his Mechanical Engineering degree from the Feng Chia University (Taiwan) in 2006 and the M.S. and Ph.D. degree on 2008 and 2014 from the National Chung-Hsing University (Taiwan), all in Mechanical Engineering. His research interests include nanofabrication, nanostructured biosensors, and MEMS/NEMS.

Ms. Fang-Ci Su received his Materials Science and Engineering degree from the Da-Yeh University (Taiwan) in 2014. The same year she became a M.S. student of the Mechanical Engineering in the National Chung-Hsing University (Taiwan).

Mr. Po-Yu Peng is a Senior Engineer of the Wafer Integration Division in the Phoenix Silicon International Corporation, Taiwan.

Dr. Hong-Tsu Young is a Distinguished Professor of the Mechanical Engineering in the National Taiwan University, Taiwan.

Mr. Stephen Liao is the Director of the Wafer Integration Division in the Phoenix Silicon International Corporation, Taiwan.

Dr. Gou-Jen Wang received the B.S. degree on 1981 from National Taiwan University and the M.S. and Ph.D. degree on 1986 and 1991 from the University of California, Los Angeles, all in Mechanical Engineering. Following graduation, he joined the Dowty Aerospace Los Angeles as a system engineer from 1991 to 1992. Dr. Wang joined the Mechanical Engineering Department at the National Chung-Hsing University, Taiwan on 1992 as an Associate Professor and has become a Professor on 1999. From 2003 to 2006, he served as the Division Director of Curriculum of the Center of Nanoscience and Nanotechnology. From 2007 to 2011, he had been the Chairman of the Graduate Institute of Biomedical Engineering, National Chung-Hsing University, Taiwan. Starting from August 2015, he has been the Dean of the College of Engineering. On 2008, he served as the Conference Chair of the Microfabrication, Integration and Packaging Conference (April/2008, Nice, France). From 2009, he is a Committee member of the Micro- and Nanosystem Division of the American Society of Mechanical Engineers. His research interests include MEMS/NEMS, biomedical micro/nano devices, nano fabrication, and tissue engineering.